A Synthetic Analogue of Rieske-Type [2Fe-2S] Clusters

Ballmann, Joachim; Albers, Antonia; Demeshko, Serhiy; Dechert, Sebastian; Bill, Eckhard; Bothe, Eberhard; Ryde, Ulf; Meyer, Franc

Published in:
Angewandte Chemie (International edition)

DOI:
10.1002/anie.200803418

2008

Document Version:
Peer reviewed version (aka post-print)

Bioinorganic Chemistry

DOI: 10.1002/anie.200((will be filled in by the editorial staff))

A Synthetic Analogue of Rieske-Type [2Fe-2S] Clusters**

*Joachim Ballmann, Antonia Albers, Serhiy Demeshko, Sebastian Dechert, Eckhard Bill, Eberhard Bothe, Ulf Ryde and Franc Meyer**

In 1964 Rieske-type [2Fe-2S] clusters were discovered in biological systems and identified as variants of [2Fe-2S] ferredoxins.[1] Structurally they differ form the parent ferredoxins by an asymmetrical terminal ligation at the [2Fe-2S] core with only one iron coordinated by two cysteinyl thiolates but the other coordinated by two histidine-N.[2] Spectroscopic (e.g. EPR and Mössbauer) and functional characteristics (namely the electrochemical potential) of Rieske-type [2Fe-2S] clusters are distinct, because of this unique coordination environment.[3] The investigation of synthetic model complexes has provided valuable insight into the properties and electronic structures of iron-sulphur cofactors.[4] While several biomimetic [2Fe-2S] clusters with all-S or all-N environment have been obtained over the last decades,[4,5] no asymmetrically ligated cluster that emulates the particular situation of the Rieske iron-sulphur proteins could be synthesized so far.[6] In the present contribution we report the synthesis and spectroscopic as well as crystallographic characterisation of the first accurate synthetic model compound **1** for Rieske-type [2Fe-2S] clusters (Scheme 1).

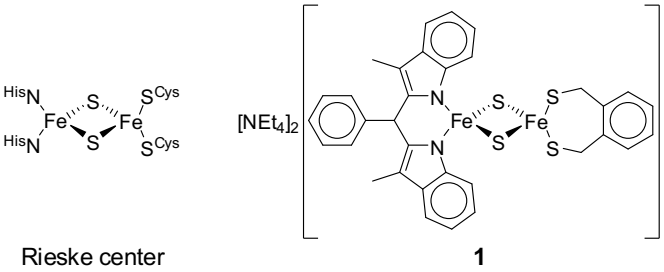

Scheme 1. Structure of the natural Rieske center and the synthetic analogue **1**.

A stepwise ligand exchange strategy starting from $[NEt_4]_2[Fe_2S_2Cl_4]$[7] seemed to be a convenient and simple approach towards a synthetic analogue of Rieske-type [2Fe-2S] sites. Closer inspection of this reaction by screening a variety of chelating $\{N_2\}$- and $\{S_2\}$-donor ligands in different combinations revealed challenging difficulties, however, such as the preferred formation of the homoleptic N- and S-coordinate compounds which where usually observed as the only products. In some cases, the sought-after asymmetrically $\{N_2S_2\}$-ligated species were detected by ESI mass spectrometry, but rapid equilibria with the corresponding homoleptic clusters prevented successful isolation of the target material. An exception was finally discovered when using a backbone phenyl substituted chelating diskatylmethane[8] capping ligand as a mimic for the natural histidine residues. In order to suppress cluster decomposition, the lithium salt of this particular $\{N_2\}$-ligand was first added to a cooled solution of $[NEt_4]_2[Fe_2S_2Cl_4]$. During optimization studies it was found advantageous to use 1.5 eq of the $\{N_2\}$ cap to ensure complete consumption of the cluster starting material, because some degradation to give monomeric N-coordinated iron complexes could not be prevented even at –40°C (fortunately, this monomeric species is readily extracted during workup). This led to the isolation of the first asymmetrically ligated [2Fe-2S] cluster $[NEt_4]_2[\{N_2\}Fe_2S_2Cl_2]$ (**2**). Minor amounts of the N-homoleptic cluster $[NEt_4]_2[\{N_2\}Fe_2S_2\{N_2\}]$ were formed as a side-product and identified by X-ray diffraction (Figure S41). Compound **2** was crystallized from DMF/diethylether, affording crystals suitable for X-ray diffraction and refinement (Figure 1). Prominent intra-core distances and angles, as well as distances and angles to the terminal coordinating atoms are in agreement with the corresponding values determined for the related homoleptic $\{N_4\}$- or $\{Cl_4\}$-ligated[7] synthetic [2Fe-2S] clusters (selected atom distances are collected in Table 1, prominent inter-atomic angles are summarized in Table S6).

With the key-intermediate **2** in hands, the intended synthetic route via subsequent exchange of the remaining two chlorine substituents proved successful. *o*-Xylene-α,α'-dithiol as $\{S_2\}$-

[*] Dipl.-Chem. J. Ballmann, A. Albers, Dr. S. Demeshko, Dr. S. Dechert, Prof. Dr. F. Meyer
Institut für Anorganische Chemie
Georg-August-Universität Göttingen
Tammannstrasse 4, 37077 Göttingen (Germany)
Fax: (+49) 551-39-3063
Phone: (+49) 551-39-3021
E-mail: franc.meyer@chemie.uni-goettingen.de
Homepage: http://www.meyer.chemie.uni-goettingen.de

Dr. E. Bill, Dr. E. Bothe
Max-Planck-Institut für Bioanorganische Chemie
Stiftstrasse 34–36, 45470 Mülheim an der Ruhr (Germany)

Prof. Dr. U. Ryde
Department of Theoretical Chemistry
Lund University
Chemical Centre, S-22100 Lund (Sweden)

[**] Financial support by the DFG (International Research Training Group GRK 1422 "Metal Sites in Biomolecules: Structures, Regulation and Mechanisms"; see www.biometals.eu) and the Fonds der Chemischen Industrie (Kekulé fellowship for J.B.) is gratefully acknowledged.

Supporting information for this article is available on the WWW under http://www.angewandte.org or from the author.

ligand[9] was selected for mimicking the biological cysteinyl thiolates, since this ligand had already been applied successfully in synthetic Fe/S chemistry.[4] Finally, cluster **1** was most conveniently obtained in a one-pot synthesis at -40°C by sequential addition of the deprotonated $\{N_2\}$-ligand prior to addition of the $Li_2\{S_2\}$-ligand salt. After extraction of the monomeric by-products (as also observed in the synthesis of intermediate **2**), the pure target material was obtained after a single re-crystallisation from DMF/diethylether. Once isolated, solid **1** is stable at RT under an atmosphere of dry dinitrogen and can even be handled in air for short periods (ca. 30 min) without decomposition. In the absence of protic solvents, solutions of **1** can be stored for weeks at RT under an atmosphere of dry dinitrogen.

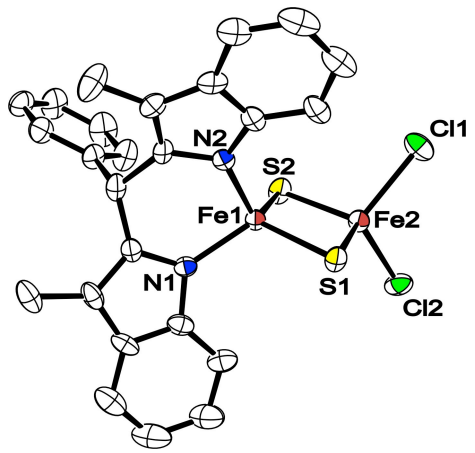

Figure 1. ORTEP plot (50% probability thermal ellipsoids) of the molecular structure of **2**. For the sake of clarity all hydrogen atoms and NEt_4^+ counter ions have been omitted. Selected atom distances (Å) and angles (°): Fe1···Fe2 2.7124(9), Fe1-N1 1.965(5), Fe1-N2 1.975(4), Fe1-S1 2.2037(13), Fe1-S2 2.2129(13), Fe2-S2 2.2088(14), Fe2-S1 2.2147(12), Fe2-Cl2 2.2490(15), Fe2-Cl1 2.2730(16), N1-Fe1-N2 93.78(17), N1-Fe1-S1 117.18(12), N2-Fe1-S1 110.58(12), N1-Fe1-S2 115.01(12), N2-Fe1-S2 116.48(10), S1-Fe1-S2 104.19(5), S2-Fe2-S1 103.97(5), S2-Fe2-Cl2 113.81(6), S1-Fe2-Cl2 109.80(5), S2-Fe2-Cl1 108.60(6), S1-Fe2-Cl1 112.49(6), Cl2-Fe2-Cl1 108.22(6), Fe1-S1-Fe2 75.74(4), Fe1-S2-Fe2 75.68(4).

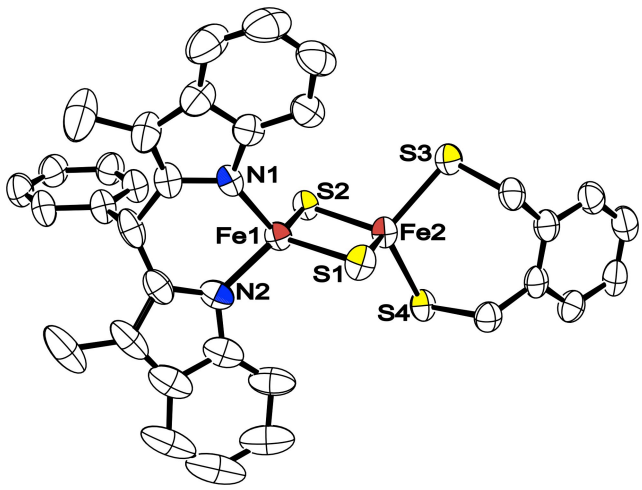

Figure 2. ORTEP plot (50% probability thermal ellipsoids) of the molecular structure of **1**. For the sake of clarity all hydrogen atoms and NEt_4^+ counter ions have been omitted. Selected atom distances (Å) and angles (°): Fe1···Fe2 2.7027(8), Fe1-N1 1.953(4), Fe1-N2 1.975(4), Fe1-S1 2.2012(14), Fe1-S2 2.2204(12), Fe2-S1 2.2228(13), Fe2-S2 2.1995(13), Fe2-S3 2.2969(14), Fe2-S4 2.2912(14), N1-Fe1-N2 94.14(16), N1-Fe1-S1 113.78(11), N2-Fe1-S1 116.82(13), N1-Fe1-S2 114.75(12), N2-Fe1-S2 113.06(11), S1-Fe1-S2 104.64(5), S2-Fe2-S1 104.61(5), S2-Fe2-S4 112.57(5), S1-Fe2-S4 108.06(5), S2-Fe2-S3 110.17(5), S1-Fe2-S3 113.21(5), S4-Fe2-S3 108.25(5), Fe1-S1-Fe2 75.31(4), Fe1-S2-Fe2 75.39(4).

Black plates suitable for X-ray diffraction were obtained by slow diffusion of diethylether into a concentrated solution of **1** in DMSO (Figure 2). **1** crystallises in the monoclinic space group C *2/c* with eight molecules per unit cell (detailed crystallographic data are presented in the electronic supporting information). Geometric parameters at both metal ions Fe1 and Fe2 are similar to the corresponding values observed for the homoleptic $\{N_4\}$- and $\{S_4\}$-ligated[9] compounds (Tables 1 and S6). Compared with the Rieske proteins, only the Fe-N distances and the N-Fe-N angles in **1** differ slightly – these differences most likely result from the protonated state of the histidine moieties in the proteins compared to the dianionic $\{N_2\}$-ligand in the model complex. Other geometric parameters perfectly agree with those found for the natural systems (see Table S7).[2c]

Table 1. Selected atom distances (Å) for **1** and **2** together with the corresponding values for the related homoleptic compounds.

compound	d (Fe···Fe)	d (Fe-S)[a]	d (Fe-N)	d (Fe-Cl)
$[\{S_2\}Fe_2S_2\{S_2\}]^{2-}$	2.698(1)	2.306(1)	---	---
ref. [9]		2.303(1)		
$[\{N_2\}Fe_2S_2\{S_2\}]^{2-}$	2.7027(8)	2.297(1)	1.953(4)	---
(**1**)		2.291(1)	1.975(4)	
$[\{N_2\}Fe_2S_2\{N_2\}]^{2-}$	2.7562(8)	---	1.975(2)	---
			1.984(3)	
$[\{N_2\}Fe_2S_2Cl_2]^{2-}$	2.7124(9)	---	1.965(5)	2.249(2)
(**2**)			1.975(4)	2.273(2)
$[Cl_2Fe_2S_2Cl_2]^{2-}$	2.716(1)	---	---	2.245(1)
ref. [7]				2.258(1)

[a] Entry refers to the terminal sulphur atoms only.

In addition to X-ray diffraction, characterisation in the solid state was completed by Mössbauer spectroscopy and magnetic susceptibility measurements. The zero-field Mössbauer spectrum of **1** is shown in Figure 3 (data summarized in Table 2). Two distinct quadrupole doublets are observed for **1**, with isomer shifts (0.26 mms^{-1} and 0.27 mms^{-1}) and quadrupole splittings (0.49 mms^{-1} and 0.98 mms^{-1}) that are in the same range as observed for the natural Rieske proteins (see Table S2). As intuitively expected, previously reported for the biological systems[10] and apparent from comparison with the homoleptic S-coordinate cluster, the larger quadrupole doublet reflects the N-coordinate Fe1 and the smaller one reflects the S-coordinate Fe2. Essentially the same considerations apply to cluster compound **2**, also ligated in an asymmetrical fashion (see Table 2, Figure S28).

Magnetic susceptibility measurements for both new complexes were carried out at a magnetic field $B = 0.5$ T from 295 to 2.0 K. Magnetic moments μ_{eff} were found in the range 0.8 - 2.3 μ_B, i.e., much lower than expected for two uncoupled ferric ($S = 5/2$) ions, and they rapidly decrease upon lowering the temperature (plots of μ_{eff} *vs.* T for **1** and **2** are shown in Figure S30 and S31, respectively). This behaviour is in accordance with strong antiferromagnetic coupling between the two ferric ions to give an $S = 0$ ground state, as is usually observed for $[2Fe\text{-}2S]^{2+}$ clusters. Coupling constants J (Table 2) were determined by using a fitting procedure to the

appropriate Heisenberg spin Hamiltonian for isotropic exchange coupling and Zeeman interaction: $H = -2JS_1 \cdot S_2 + g\mu_B(S_1 + S_2) \cdot B$. Interestingly, J values for both asymmetrically coordinated compounds **1** and **2** indicate an increased antiferromagnetic coupling compared to the related homoleptic $\{N_4\}$- or $\{Cl_4\}$-ligated clusters.

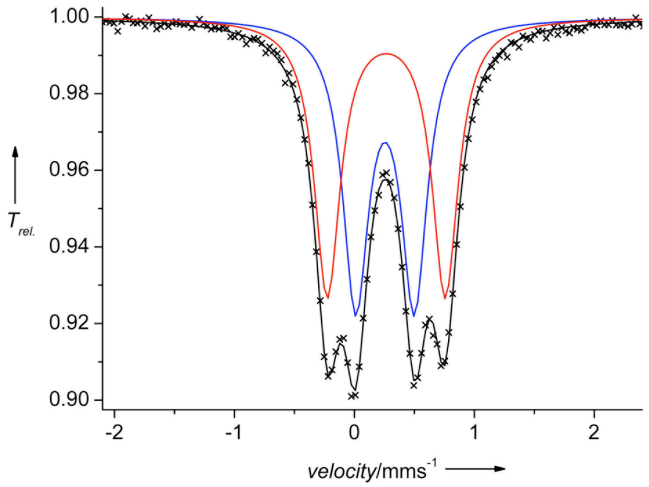

Figure 3. Zero-field Mössbauer spectrum of **1** recorded at 80 K. Isomer shifts and quadrupole splittings are summarized in Table 2.

All new [2Fe-2S] cluster compounds were additionally characterized in solution by UV-Vis, ^{1}H NMR spectroscopy and ESI mass spectrometry. Assignment of the partially overlapping electronic absorption bands remains somewhat speculative, and more detailed analyses will be required to locate the different charge-transfer transitions (see Figures S4 – S7). Reasonably well resolved ^{1}H NMR spectra could be recorded because of the strong antiferromagnetic coupling, and signal sets for the $\{N_2\}$-ligand and the $\{S_2\}$-ligand can be clearly distinguished (see Figure S25). Positive and negative ion ESI mass spectra for all cluster compounds show dominant signals for $[M+NEt_4]^+$ and $[M–NEt_4]^–$, respectively (all spectra, including high resolution ESI(+) spectra are depicted in the electronic supporting information in Figures S8 – S24).

Table 2. Analytical data for cluster **1** and **2** together with the corresponding data for the related homoleptic compounds.

Cluster	δ (ΔE_Q) [a] / mms^{-1}	J [b] / cm^{-1}	$E_{1/2}$ [c] / V
$[\{S_2\}Fe_2S_2\{S_2\}]^{2-}$ [d]	0.28 (0.36)	–149±8	–1.51 [e]
$[\{N_2\}Fe_2S_2\{S_2\}]^{2-}$ (**1**)	0.26 (0.49), 0.27 (0.98)	–161	–1.35
$[\{N_2\}Fe_2S_2Cl_2]^{2-}$ (**2**)	0.32 (0.99), 0.32 (0.72)	–184	–1.25 [f]
$[Cl_2Fe_2S_2Cl_2]^{2-}$ [g]	0.37 (0.82) [h]	–158	–1.02 [i]

[a] ^{57}Fe Mössbauer parameters at 80 K relative to iron metal at RT. [b] Values obtained from fits to SQUID data. [c] Potentials in DMF/0.1 M NBu_4PF_6 at a scan rate of 100 mV/s *vs.* the $Cp^*_2Fe/Cp^*_2Fe^+$ couple. [d] Reference 9. [e] Half-wave potential $E_{1/2}$ in DMF *vs.* SCE is –1.49 V, corresponding to –1.51 V *vs.* the $Cp^*_2Fe/Cp^*_2Fe^+$ couple. [f] cathodic peak potential of the irreversible process. [g] Reference 7. [h] this work (Figure S29). [i] cathodic peak potential of the irreversible process recorded in MeCN/0.1 M NBu_4Cl *vs.* SCE is –1.00 V, corresponding to –1.02 V *vs.* the $Cp^*_2Fe/Cp^*_2Fe^+$ couple.

Redox properties of all new complexes were studied by cyclic voltametry in DMF/0.1 M NBu_4PF_6 solution at RT. The Rieske-type cluster **1** exhibits a reversible one-electron reduction at –1.35 V *vs.* decamethylferrocene and a second irreversible reduction wave at approximately –2.0 V corresponding to formation of the all-ferrous species. Thus, the half-wave potential corresponding to the $[2Fe\text{-}2S]^+/[2Fe\text{-}2S]^{2+}$ pair of **1** is shifted slightly positive compared to the one-electron reduction wave observed for the homoleptic $\{S_4\}$-ligated analogue (–1.51 V)[7a]. As expected, the unusual high redox potentials of the biological Rieske sites are not reflected by the model cluster **1**, due to the dianionic character of the coordinated $\{N_2\}$-ligand instead of the protonated neutral histidine residues. Since this first-generation synthetic model cannot undergo the same deprotonation-assisted electron transfer as the natural counterpart, which relies on the peripheral histidine-N as protonation sites,[11] a dependence of the redox potential on the presence of proton sources is ruled out. Reduction of **2** is irreversible on the timescale of the cyclic voltametry, as also observed for the homoleptic Cl_4-ligated cluster[7c] (electrochemical data are summarized in Table 2, voltamograms are shown in Figure S32 and Figure S33).

The one-electron reduced mixed-valent species of **1** was generated in MeCN solution by constant potential coulometry (CPC) at –25°C. Reduction was carried out at –1.9 V *vs.* the Cp_2Fe/Cp_2Fe^+ couple, corresponding to –1.39 V *vs.* $Cp^*_2Fe/Cp^*_2Fe^+$. The progress was followed by UV-Vis spectroscopy (Figure 4), recorded every 1.5 min directly in the coulometric cell and stopped after a charge consumption of approximately 300 mC (calculated for one-electron reduction: 304 mC, see Figure S35). Over the time of the coulometric experiment (overall ~13.5 min), intensities of the main visible bands decreased with two isosbestic points present. Cyclic voltamograms before and after coulometry (Figure S34) were nearly identical in terms of peak potentials, intensities and the overall line shapes, indicating that the redox process is reversible on the voltametry and the coulometry timescale.

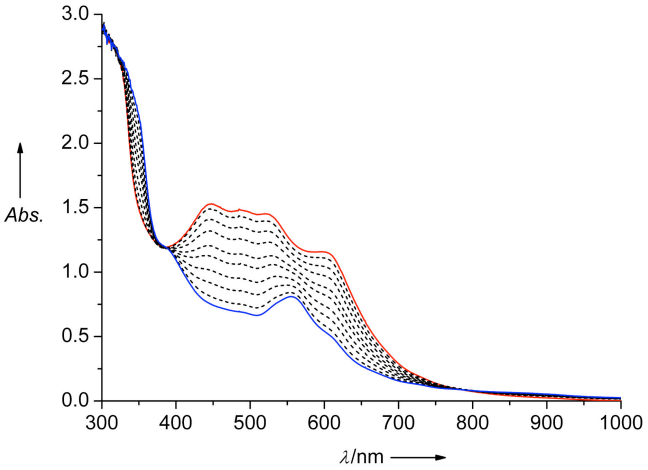

Figure 4. UV-Vis spectra recorded during constant potential coulometry of **1** at –25°C, –1.9 V *vs.* Cp_2Fe/Cp_2Fe^+, red line: t_0 = 0 min, dotted lines and blue line (after ~ 13.5 min): $t_0 + n\,\Delta t$, Δt = 1.5 min, n = 1 - 9, c = 3.94×10^{-4} M in MeCN/0.2 M NBu_4PF_6.

Samples for EPR spectroscopy were taken after ~50% reduction (Figure 5) and after 100% reduction, and were immediately frozen in liquid dinitrogen. A characteristic low g_3 value, as detected for the reduced $[2Fe\text{-}2S]^+$ cluster in Rieske proteins[12] (g_3 ~ 1.78 - 1.81) was observed for the 50% reduced sample by fitting the experimental EPR data with $g_1 = 2.014$, $g_2 = 1.936$ and $g_3 = 1.804$, while g_1 is slightly lower and g_2 somewhat higher than the

corresponding values found for Rieske proteins ($g_1 \sim 2.02$ - 2.03, $g_2 \sim 1.89$ - 1.90).[3a,13] The low averaged $g_{av} = 1.918$ for **1** (compare $g_{av} = 1.90$ - 1.91 for Rieske proteins[3a,13] and $g_{av} = 1.95$ - 1.97 for ferredoxins;[14] g values of selected proteins are collected in Tables S3 and S4) and the wide anisotropy of the main components of the g tensor (mainly a result of the low g_3 value) suggest, that reduction takes place at the N-ligated iron atom of **1**. This lowering of g_3 and g_{av} in Rieske-type $[2Fe\text{-}2S]^+$ species was previously attributed to a more pronounced orthorhombic C_{2v} distortion at the $\{N_2S_2\}$-surrounded tetrahedral ferrous iron.[15]

An improved overlap of the experimental values with the fit curve is observed for the 100% reduced sample with virtually identical g values measured for the target material ($g_1 = 2.015$, $g_2 = 1.936$, $g_3 = 1.803$). However, a second, as yet unknown species (~12%, delocalized $S = ½$ radical, fitted with $g_1 = 2.096$, $g_2 = 2.021$ and $g_3 = 1.906$) formed during the 100% CPC, probably due to some over-reduction (Figure S37). The reduced $[2Fe\text{-}2S]^+$ species seems to be slightly instable, also indicated by an increasing UV-Vis absorption after completed coulometry (measured 3.5 min after 100% CPC, no electrical current applied to the sample, but kept under argon at –25°C, see Figure S36).

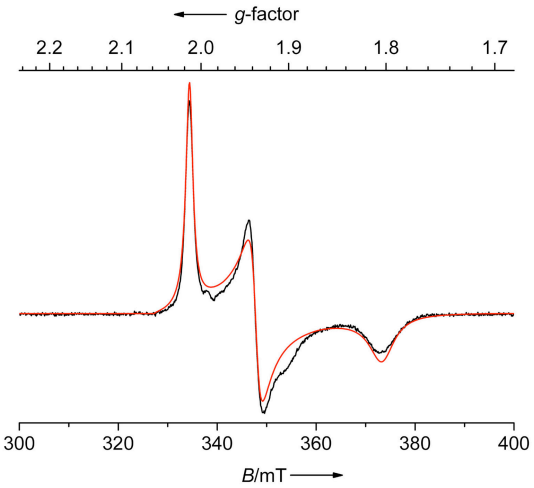

Figure 5. EPR spectrum of the one-electron reduced **1** (generated *via* constant potential coulometry at –25°C, –1.9 V *vs.* Cp_2Fe/Cp_2Fe^+, sample taken after ~ 50% reduction), recorded at 20 K in frozen MeCN/0.2 M NBu_4PF_6 ($c = 3.94\times10^{-4}$ M, spectrometer frequency: 9.43198 GHz, microwave power 25 μW, modulation amplitude: 1 mT).. The red line is fitted to the experimental values (black line) with $g_1 = 2.014$, $g_2 = 1.936$ and $g_3 = 1.804$.

In order to corroborate conclusions from the EPR findings, DFT calculations were carried out with the Turbomole 5.9 software package,[16a] using the Becke-Perdew-1986 functional (BP86)[16b,c] and the def2-SVP[16d] basis set. Both the oxidized and reduced form of **1** were studied in the antiferromagnetically coupled spin state. Analysis of the molecular orbitals revealed a localization of the LUMO in oxidized **1** (Figure S43) at the N-coordinate Fe atom. Accordingly, the HOMO in reduced **1** (Figure 6) is located at this unique iron, as previously concluded form DFT calculations on a fictive mixed-valent Rieske-type model system.[16e]

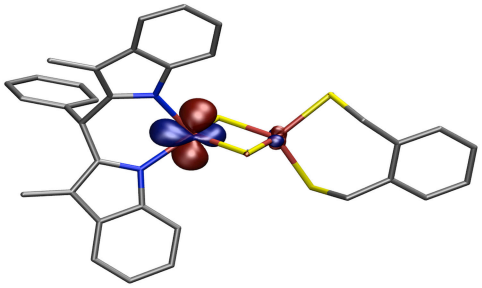

Figure 6. Illustration of the highest occupied molecular orbital (HOMO, contour value = 0.06) of **1** in the one-electron reduced mixed-valent state. Hydrogen atoms are omitted for clarity.

In conclusion, the first exact synthetic model for [2Fe-2S] Rieske sites reported here adequately emulates structural, Mössbauer, and EPR parameters of the analogous protein-bound clusters. Future efforts will focus on the incorporation of additional nitrogen atoms into the $\{N_2\}$-ligand backbone, in order to provide potential protonation sites that would allow to more closely mimic the electrochemical properties of the natural enzymes and to support the role of the iron-ligated histidines in the pH-dependence of the reduction potential.[11]

Received: ((will be filled in by the editorial staff))
Published online on ((will be filled in by the editorial staff))

Keywords: bioinorganic chemistry · iron · sulphur · Rieske · Mössbauer spectroscopy

[1] a) J. S. Rieske, D. H. MacLennan, R. Coleman, *Biochem. Biophys. Res. Commun.* **1964**, *15*, 338-344; b) J. S. Rieske, *J. Biol. Chem.* **1968**, *239*, 3017-3022.

[2] a) T. A. Link, M. Saynovits, C. Assmann, S. Iwata, T. Ohnishi, G. von Jagow, *Eur. J. Biochem.* **1996**, *237*, 71-75; b) S. Iwata, M. Saynovits, T. A. Link, H. Michel, *Structure* **1996**, *4*, 567-579; c) H. Bönisch, C. L. Schmidt, G. Schäfer, R. Ladenstein, *J. Mol. Biol.* **2002**, *319*, 719-805; d) T. A. Link, O. M Hatzfeld, M. Saynovits, *Bioinorg. Chem.* **1997**, 312-325.

[3] a) J. A. Fee, K. L. Findling, T. Yoshida, R. Hille, G. E. Tarr, D. O. Hearshen, W. R. Dunham, E. P. Day, T. A. Kent, E. Münck, *J. Biol. Chem.* **1984**, *259*, 124-133; b) D. J. Ferraro, L. Gakhar, S. Ramaswamy, *Biochem. Biophys. Res. Commun.* **2005**, *338*, 175-190.

[4] P. V. Rao, R. H. Holm, *Chem. Rev.* **2004**, *104*, 527-559.

[5] a) D. Coucouvanis, A. Salifoglou, M. G. Kanatzidis, A. Simopoulos, V. Papaefthymiou, *J. Am. Chem. Soc.* **1984**, *106*, 6081-6082.; b) J. Ballmann, X. Sun, S. Dechert, E. Bill, F. Meyer, *J. Inorg. Biochem.* **2007**, *101*, 305-312.

[6] few symmetrical [2Fe-2S] clusters with mixed {NS} ligand set at each iron have been reported: a) P. Beardwodd, J. F. Gibson, *J. Chem. Soc. Dalton Trans.* **1992**, 2457-2466; b) Y. Ohki, Y. Sunada, K. Tatsumi, *Chem. Lett.* **2005**, *34*, 172-173.

[7] a) M. A. Bobrik, K. O. Hodgson, R. H. Holm, *Inorg. Chem.* **1977**, *16*, 1851-1858; b) Y. Do, E. D. Simhon, R. H. Holm, *Inorg. Chem.* **1983**, *22*, 3809-3812; c) G. B. Wong, M. A. Bobrik, R. H. Holm, *Inorg. Chem.* **1978**, *17*, 578-584.

[8] K. Dittmann, U. Pindur, *Arch. Pharm.* **1985**, *318*, 340-350.

[9] a) J. J. Mayerle, S. E. Denmark, B. V. DePamphilis, J. A. Ibers, R. H. Holm, *J. Am. Chem. Soc.* **1975**, *97*, 1032-1045; b) W. O. Gillum, R. B. Frankel, S. Foner, R. H. Holm, *Inorg. Chem.* **1976**, *15*, 1095-1100.

[10] a) J. A. Fee, K. L. Findling, T. Yoshida, R. Hille, G. E. Tarr, D. O. Hearshen, W. Dunham, E. P. Day, T. A. Kent, E. Münck, *J. Biol. Chem.* **1984**, *259*, 124-133; b) D. Kuila, J. A. Fee, *J. Biol. Chem.* **1986**,

261, 2768-2771; c) P. J. Geary, D. P. E. Dickson, *Biochem. J.* **1981**, *195*, 199-203.

[11] a) D. J. Kolling, J. S. Brunzelle, S Lhee, A. R. Crofts, S. K. Nair, *Structure* **2007**, *15*, 29-38; b) T. Iwasaki, A. Kounosu, D. R. J. Kolling, A. R. Crofts, S. A. Dikanov, A. Jin, T. Imai, A. Urushiyama, *J. Am. Chem. Soc.* **2004**, *126*, 4788-4789; c) N. J. Cosper, D. Matthew, A. Kounosu, N. Kurosawa, E. L. Neidle, D. M. Kurtz Jr., T. Iwasaki, R. A. Scott, *Prot. Sci.* **2002**, *11*, 2969-2973; d) Y. Zu, M. M.-J. Couture, D. R. J. Kolling, A. R. Crofts, L. D. Eltis, J. A. Fee, J. Hirst, *Biochemistry* **2003**, *42*, 12400-12408; e) A. R. Klingen, G. M. Ullmann, *Biochemistry* **2004**, *43*, 12383-12389; f) E. J. Leggate, J. Hirst, *Biochemistry* **2005**, *44*, 7048-7058; g) I-J. Lin, Y. Chen, J. A. Fee, J. Song, W. M. Westler, J. L. Markley, *J. Am. Chem. Soc.* **2006**, *128*, 10672-10673.

[12] a) M. Rampp, E. Kellner, A. Müller, A. Riedel, *Bioinorg. Chem.* **1997**, 295-301; b) M. K. Bowman, E. A. Berry, A. G. Roberts, D. M. Kramer, *Biochemistry* **2004**, *43*, 430-436.

[13] a) J. N. Siedow, S. Power, F. F. De la Rosa, G. Palmer, *J. Biol. Chem.* **1978**, *263*, 2392-2399; b) S. De Vries, S. P. J. Albracht, F. I. Leeuwerik, *Biochim. Biophys. Acta* **1979**, *546*, 316-333; c) R. C. Prince, *Biochim. Biophys. Acta* **1983**, *723*, 133-138; d) R. Malkin, A. J. Bearden, *Biochim. Biophys. Acta* **1978**, *505*, 147-181; e) B. L. Trumpower, C. A. Edwards, T. Ohnishi, *J. Biol. Chem.* **1980**, *92*, 209-223; f) F. T. de Oliveira, E. L. Bominaar, J. Hurst, J. A. Fee, E. Münck, *J. Am. Chem. Soc.* **2004**, *126*, 5338-5339.

[14] a) J. Fritz, R. Anderson, J. Fee, G. Palmer, R. H. Sands, J. C. M. Tsibris, I. C. Gunsalus, W. H. Orme-Johnson, H. Beinert, *Biochim. Biophys. Acta* **1971**, *253*, 110-133; b) D. V. Devartanian, Y. I. Shethna, H. Beinert, *Biochim. Biophys. Acta* **1969**, *194*, 548-563; c) J. A. Fee, G. Palmer, *Biochim. Biophys. Acta* **1971**, *245*, 175-195; d) K. Mukai, T. Kimura, J. Helbert, L. Kevan, *Biochim. Biophys. Acta* **1973**, *295*, 49-56; e) P. Bertrand, J. P. Gayda, *Biochim. Biophys. Acta* **1979**, *579*, 107-121.

[15] P. Bertrand, B. Guigliarelli, J.-P. Gayda, P. Beardwood, J. F. Gibson, *Biochim. Biophys. Acta* **1985**, *831*, 261-266.

[16] a) R. Ahlrichs, M. Bär, M. Häser, H. Horn, C. Kölmel, *Chem. Phys. Lett.* **1989**, *162*, 165-169; b) A. D. Becke, *Phys. Rev. A* **1988**, *38*, 3098-3100; c) J. P. Perdew, *Phys. Rev. B* **1986**, *33*, 8822-8824; d) F. Weigend, R. Ahlrichs, *Phys. Chem. Chem. Phys.* **2005**, *7*, 3297-3305; e) M. Shoji, K. Koizumi, Y. Kitagawa, S. Yamanaka, M. Okumura, K. Yamaguchi, *Int. J. Quantum Chem.* **2007**, *107*, 609-627.

Entry for the Table of Contents

Bioinorganic Chemistry

Joachim Ballmann, Antonia Albers, Serhiy Demeshko, Sebastian Dechert, Eckhard Bill, Eberhard Bothe, Ulf Ryde and Franc Meyer*

_____ **Page – Page**

A Synthetic Analogue of Rieske-Type [2Fe-2S] Clusters

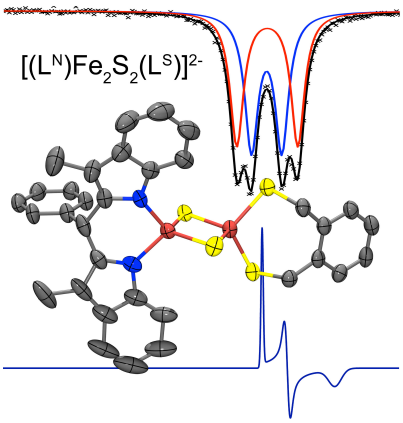

An accurate synthetic model for Rieske-type [2Fe-2S] cluster has been prepared that emulates structural and spectroscopic features of the natural protein sites, including the characteristic low g_{av} value in the EPR spectra of the reduced $[2Fe\text{-}2S]^+$ species.